第 33 卷第 2 期
2017 年 2 月

无 机 化 学 学 报
CHINESE JOURNAL OF INORGANIC CHEMISTRY

Vol.33 No.2
243-248

硫与 Mn_2O_3 空心球的复合结构及其在锂硫电池中的应用

王 瑛[1] 弭 侃[2] 熊胜林*,[2]

([1]山东玉皇新能源科技有限公司,菏泽 274000)

([2]山东大学化学与化工学院,济南 250100)

摘要：在水热条件下，以碳球为模板合成了 Mn_2O_3 空心球，并用作锂硫电池的载硫基底材料。测试结果表明载硫量为 51%的 Mn_2O_3-S 复合材料显示了较高的比容量,良好的循环稳定性和倍率性能。循环 100 圈后,最终可逆容量仍保持 657 mA·g^{-1},证明该 Mn_2O_3 空心球是一种有潜力的载硫基底材料。

关键词：电化学；空心球；三氧化二锰；锂硫电池

中图分类号：O614.71^{+}1；O613.51 **文献标识码**：A **文章编号**：1001-4861(2017)02-0243-06

DOI:10.11862/CJIC.2017.048

Immobilizing Sulfur in Mn_2O_3 Hollow Spheres for Lithium-Sulfur Batteries

WANG Ying[1] MI Kan[2] XIONG Sheng-Lin*,[2]

([1]*Shandong Yuhuang New Energy Technology Co., LTD, Heze, Shandong* 274000, *China*)

([2]*School of Chemistry and Chemical Engineering, Shandong University, Jinan* 250100, *China*)

Abstract: Uniform Mn_2O_3 hollow spheres were synthesized by using carbon spheres as the hard template and were used as holder for Li-S batteries. The Mn_2O_3-S composites showed a high specific capacity, good cycling stability and rate performance. The final reversible capacity can remain at 657 mA·g^{-1} after 100 cycles at the current density of 0.9 A·g^{-1} with the 51% sulfur loading, which demonstrates that Mn_2O_3 hollow spheres could be a promising matrix for Li-S batteries.

Keywords: electrochemistry; hollow spheres; manganic oxide; Li-S batteries

0 Introduction

In recent years, Lithium-sulfur batteries are receiving increasing attentions from all around the world due to its numerous advantages, including its low cost, nontoxic nature and remarkable theoretical specific capacity and energy density (1 675 mAh·g^{-1} and 2 500 Wh·kg^{-1}). However, the practical application of Li-S batteries is still hindered by many problems. For example, the insulation of sulfur can lower the electrochemical utilization of active material and lead to the poor rate capability. What is more, the dissolution of intermediate discharge products (Li_2S_x, $3 < x < 9$) can result in the poor cycling performance and Coulombic efficiency of cell[1-7].

To overcome these issues of Li-S batteries, a lot of schemes have been carried out to improve the corresponding electrochemical performance. First, carbon materials with different morphology (like hollow carbon spheres[8-10], mesoporous carbon spheres[11-13] or nanotubes[14], and graphene[15-17] and so on) have been designed for the holder of sulfur in consideration of

收稿日期:2016-09-01。收修改稿日期:2016-11-17。

山东省自然科学杰出青年基金(No.JQ201304)资助项目。

*通信联系人。E-mail:chexsl@sdu.edu.cn

the excellent conductivity and the advantageous pore structure which favors suppressing the loss of sulfur and the discharge produces. As a result, the related cycling performance and reversible capacity of composites with sulfur are obviously enhanced. However, the capacity of Li-S batteries is still decayed during the long-term electrochemical cycle, which may be attributed to the nonpolar nature of carbon. Recently, besides pure carbon matrix, the polar metal oxides (like TiO_2[18-19], Al_2O_3[20], V_2O_5[21], MnO_2[22-23] and so on) are reported as holder or absorber for Li-S batteries. Due to that the dissolution of polysufides is effectively buffered by the surficial chemical adsorption of metal oxides, the enhanced cycling performances are obtained. It is no doubt that the cycling stability of cells is largely improved by the usage of those metal oxides.

In this paper, Mn_2O_3 hollow spheres were developed with purpose to incorporate sulfur, which were synthesized by using carbon spheres as hard template. When evaluated as cathode in Li-S batteries, Mn_2O_3-S composites exhibited a reversible capacity of 657 $mAh \cdot g^{-1}$ after 100 cycles at the current density of 900 $mA \cdot g^{-1}$.

1 Experimental

1.1 Synthesis of carbon spheres and Mn_2O_3 hollow spheres

Firstly, carbon spheres were synthesized by a modified method[24]. Typically, 3.83 g glucose and 0.27 g cetyl trimethyl ammonium bromide (CTAB) was dissolved totally in 40 mL of deionized water. Then, the solution was transferred into a 65 mL Teflon-lined autoclave and heated for 9 h at 180 ℃. The final product was collected by centrifugation with water and ethanol for several times. To produce the Mn_2O_3 hollow spheres, 0.15 $mol \cdot L^{-1}$ manganese acetate solution was formed with 40 mL of absolute ethanol as the solvent. After the PH was adjusted to be 5 by hydrochloric acid, 0.5 g of carbon spheres was introduced into the above solution and then followed by ultrasonic treatment for about 2 h. The final mixture was centrifuged by water and ethanol before it was aged for 8 h at 50 ℃ in an oven. The powder was dried at 60 ℃ for overnight and finally heated at 500 ℃ for 2.5 h with a heating ratio of 2 $℃ \cdot min^{-1}$ to attain Mn_2O_3 hollow spheres.

1.2 Preparation of Mn_2O_3-S composites

In a typical synthesis, sulfur and Mn_2O_3 hollow spheres were mixed with the mass ratio of 55∶45. Then, a moderated amount of CS_2 was added and stirred until it was evaporated completely. Finally, the mixture was heated at 155 ℃ for 10 h to get the Mn_2O_3-S composites.

1.3 Sample characterization

TEM and SEM images were obtained from a transmission electron microscope (TEM, JEM-1011, Japan) and a scanning electron microscope (SEM, JSM -7600F, Japan), respectively. X-ray powder diffraction (XRD) pattern was examined on a Bruker D8 advance X-ray diffractometer with Cu $K\alpha$ as a radiation (λ= 0.154 18 nm, U=40 kV, I=40 mA, 2θ=8°~80°). The sulfur content of Mn_2O_3/S composites was collected from a Mettler Toledo TGA/SDTA851 thermal analyzer with a heating rate of 5 $℃ \cdot min^{-1}$ under a nitrogen atmosphere. The chemical analysis of the samples was performed using X-ray photoelectron spectroscopy (XPS, ESCALAB 250 spectrometer, Perkin-Elmer).

1.4 Electrochemical measurements

Typically, 75% of Mn_2O_3-S composites, 15% of carbon black, and 10% of polyvinylidene fluoride (PVDF) (mass ratio =75∶15∶10) were mixed in *N*-methylpyrrolidinone (NMP) to form a slurry and coated on aluminum foil to prepare the cathode. The foil was cut into discs with the diameter of 12 mm and the areal mass of sulfur for each disc is about 1.0~1.2 $mg \cdot cm^{-2}$. The discs were assembled with a Li metal foil as the counter electrode and the Celgard 2400 as the separator. All cells were assembled in an argon-filled glovebox. The electrolyte used was 1 $mol \cdot L^{-1}$ bis (trifluoromethane) sulfonamide lithium salt (LiTFSI) in a mixed solvent of 1,3-dioxolane (DOL) and 1,2-dimethoxyethane (DME) (the volumetric ratio of 1∶1) with 2% $LiNO_3$ to prohibit the shuttle effect. The charge-discharge behaviors were tested in a potential window of 1.7~2.8 V at 30 ℃ by using a LAND

CT2001A instrument. The Cyclic voltammograms (CV) were obtained from an LK2005A electrochemical workstation at a scan rate of 0.1 $mV \cdot s^{-1}$.

2　Results and discussion

2.1　Structure characterization

Fig.1a indicates TEM image of carbon spheres, which were synthesized by the hydrothermal method using glucose as precursor. It can clearly seen that the sizes of those carbon spheres were ranging from 500 to 700 nm. The hydrophilic surface of carbon spheres renders lots of functional groups (like hydroxyl) which could adsorb Mn^{2+} from the ethanol solution. After calcination and removal of carbon spheres, Mn_2O_3 hollow spheres were obtained (the corresponding XRD was displayed in Fig.2). TEM image in Fig.1b demonstrates the hollow structure of the as-prepared Mn_2O_3 spheres with the thickness of the shell about 30 nm. As shown in Fig.1c, the panoramic SEM image reveals the large area of uniform spheres with diameters of 300~500 nm. Fig. 1d shows SEM image of Mn_2O_3-S composites. It is clear that the sphere structure of Mn_2O_3 was still remained even after the sulfur was infiltrated into Mn_2O_3 hollow spheres. More importantly, the massive sulfur aggregates were hardly observed on the surface of composites, which revealed that the uniform dispersion of sulfur in the oxide matrix.

The XRD patterns of Mn_2O_3 hollow spheres and Mn_2O_3-S composites are indicated in Fig.2a. The characteristic diffraction peaks of the product after calcination process in laboratory air matched perfectly with cubic Mn_2O_3 (JCPDS Card No.65-7467). As for the Mn_2O_3-S composites, the intensity of sulfur diffraction peaks becomes obviously lower than that of pure elemental sulfur, which suggests the sulfur has been distributated well into Mn_2O_3 hollow spheres and concides with the above FESEM observation. The TGA calculations reveal that the actual mass ratio of sulfur in the Mn_2O_3-S composites is approximately 51% (Fig.2b).

Fig.3 showed the XPS spectra of S2*p* and Mn2*p* of Mn_2O_3-S composites. From Fig.3a, the spectrum of S2*p* was divided into two sets of peaks. The peaks located at 163.8 and 164.9 eV are the typical signals of pure S, while the other two peaks loacted at 168.4

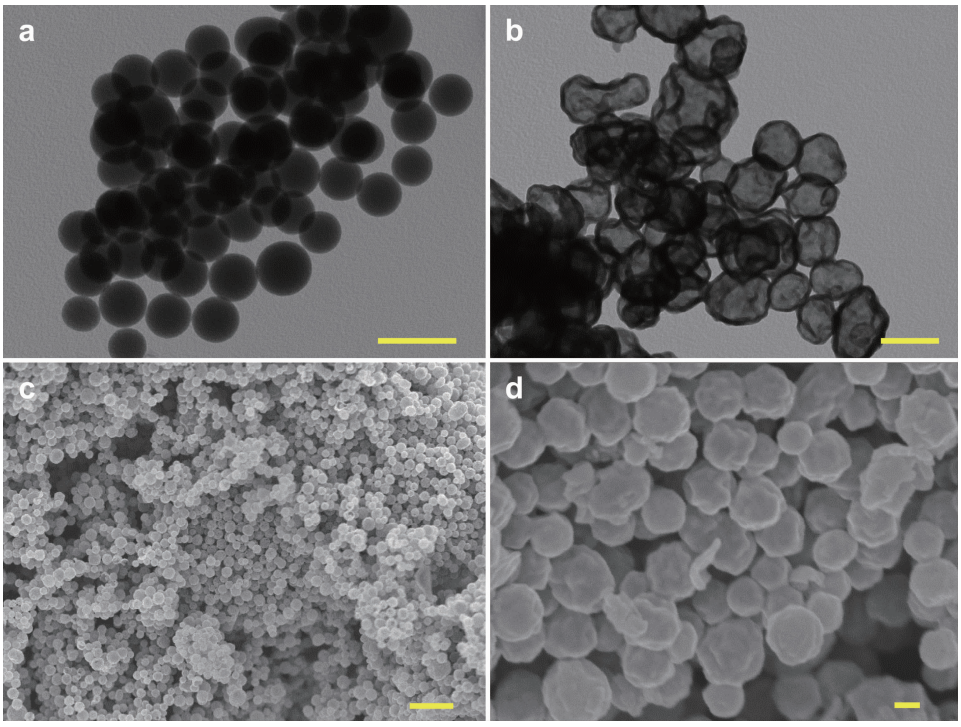

Scale bars: (a) 1 μm; (b) 250 nm; (c) 1 μm; and (d) 100 nm

Fig.1　(a) TEM image of carbon sphere; (b, c) TEM and SEM images of Mn_2O_3 hollow spheres; (d) SEM image of Mn_2O_3-S composites

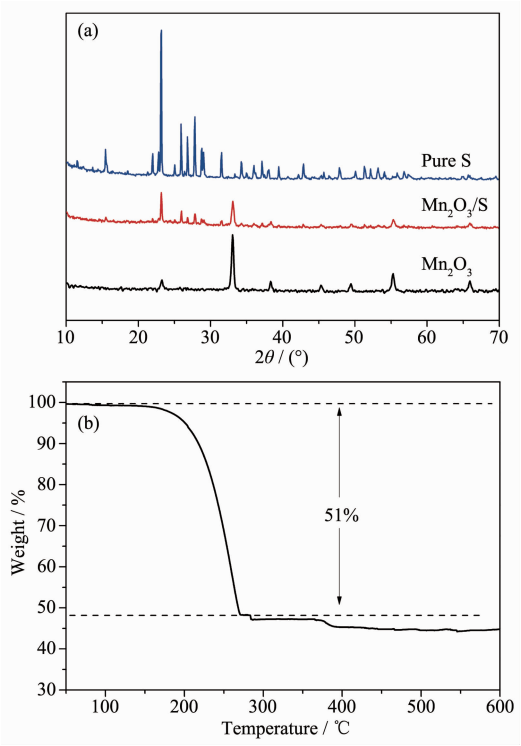

Fig.2 (a) XRD patterns of pure sulfur, Mn_2O_3 hollow spheres and Mn_2O_3-S composites; (b) TGA curve of the Mn_2O_3-S composites

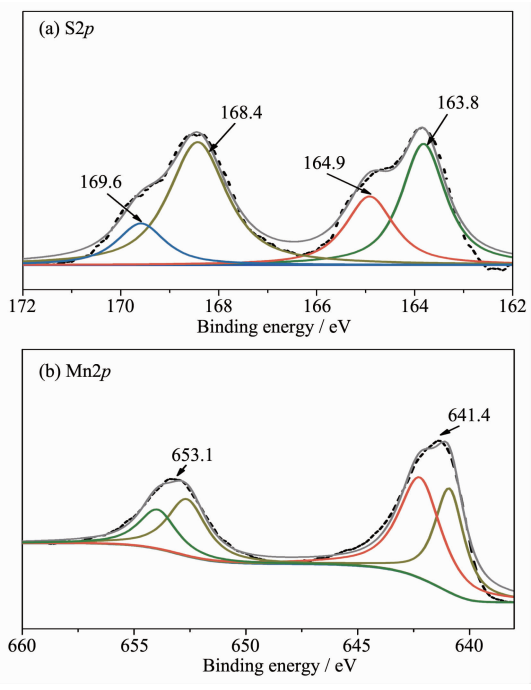

Fig.3 XPS spectra of S2*p* (a) and Mn2*p* (b) of Mn_2O_3-S composites

and 169.6 eV were characteristic of SO_x species, which may be caused by Mn_2O_3 covalently bonding with S[23]. In addition, the binding energies of Mn2$p_{3/2}$ and Mn2$p_{1/2}$ in Fig.3b are 641.4 and 653.1 eV, which can be attributed to the spin-orbit splitting. Like some literatures reported, the binding energy difference between Mn2$p_{1/2}$ and Mn2$p_{3/2}$ is 11.7 eV, indicating the existence of Mn^{3+} in Mn_2O_3-S composites[25-26]. It is worth noting that the signals of Mn2*p* peaks displayed an apparent shift to the lower binding energy, which is related with an increased electron cloud density from the adjacent sulfur element[23].

2.2 Electrochemical performance

The electrochemical property of the as-fabricated product was first investigated by cyclic voltammetry. Fig.4 indicates the first five consecutive cyclic voltammograms (CVs) of the electrode made from Mn_2O_3-S composites. Two reduction peaks can be found in the cathodic polarization process of the first cycle. The first reductive peak located at 2.3 V can be assigned to the conversion of element sulfur (S_8) to long-chain lithium polysulfides (Li_2S_x, $5 < x < 8$). The second reductive peak at 2.0 V suggests the further decomposition of the soluble lithium polysulfides to insoluble short-chain lithium sulfides (Li_2S_2 and/or Li_2S). During the following anodic scan, there is only one obvious oxidation peak at 2.45 V, which is associated with the slow oxidation of Li_2S or Li_2S_2 to long-chain lithium polysulfides[4]. From the second cycle onwards, the CV curves mostly overlap, showing the good reversibility of the electrochemical reactions. In addition, it is clear that there′re other peaks in the CV curves

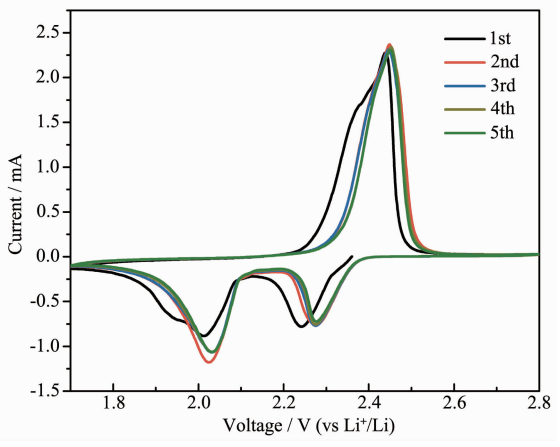

Fig.4 First five consecutive CVs of the electrode made from Mn_2O_3-S composites at a scan rate of 0.1 $mV \cdot s^{-1}$

except the above peaks, which reveals that Mn_2O_3 matrix can not participate in the electrochemical reaction in the voltage window of 1.7~2.8 V.

Fig.5a indicates the typical discharge-charge voltage profiles of the Mn_2O_3-S composites at a current density of 0.9 A·g^{-1}. There are two typical plateaus located at 2.3 and 2.1 V in the curves, which are in agreement with the above CV observation. Fig.5b shows the cycling performance of Mn_2O_3-S electrode was measured at the current density of 0.9 A·g^{-1}. When the sulfur mass in the composites is 51%, the Mn_2O_3-S electrode delivers high first-cycle discharge and charge capacities of 1 003.3 and 989.5 mAh·g^{-1} respectively, corresponding to a Coulombic efficiency

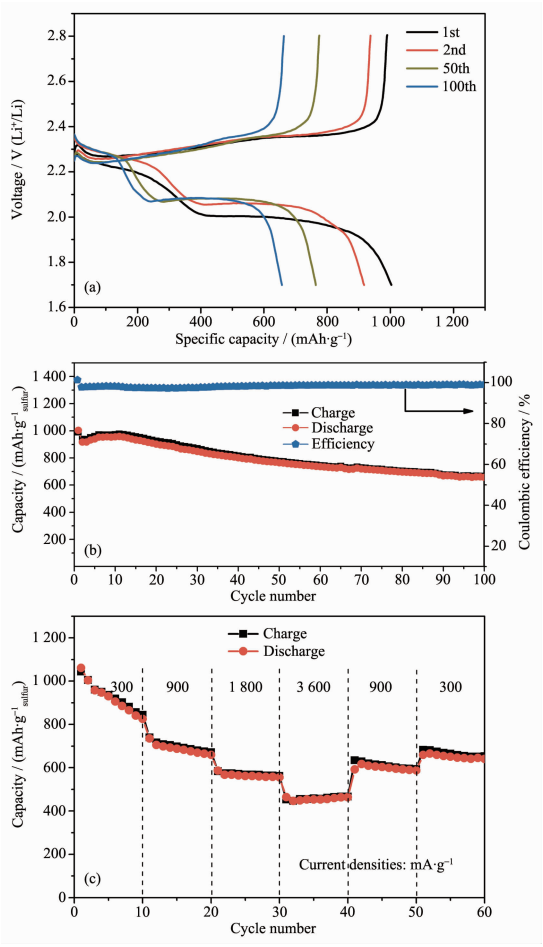

Fig.5　Electrochemical performance of Mn_2O_3-S composites: (a) cycling performance at a current density of 0.9 A·g^{-1} and the corresponding Coulombic efficiency; (b) discharge-charge voltage profiles for the 1st, 2nd, 50th, and 100th cycles at a current density of 0.9 A·g^{-1}; (c) rate performance at various current rates

(CE) of 101.4%. A discharge capacity of 917.1 mAh·g^{-1} is delivered in the second cycle, followed by a charge capacity of 937.2 mAh·g^{-1}, resulting in a high CE of about 97.9%. Furthermore, the final discharge capacity can remained at 657 mAh·g^{-1} after 100 cycles. Although the reversible capacity is still decaying during the cycling process, which may attributed to some soluble polysulfides escaped from the Mn_2O_3 matrixes and dissolved into the electrolyte, The final retention of reversible capacity can still remain at 65.5%. In addition, the CE can keep approximately 100% during the discharge-charge process, which suggested the good reversibility of the Mn_2O_3-S materials. The rate performance was also tested at various rates (Fig.5c). As can be seen, the reversible capacities are 1 061, 735, 586, 464 mAh·g^{-1} at the current density of 0.3, 0.9, 1.8, 3.6 A·g^{-1}, respectively, which reveals that the Mn_2O_3-S electrode has the good electrochemical performance even at the high rates. When the rate went back to 0.9 and 0.3 A·g^{-1} after 40 cycles, the corresponding capacities can remain at 592 and 659 mAh·g^{-1}, receptively. Furthermore, both the discharge and charge capacities could be stable at different current densities and the CE was almost 100%, indicating a good inhibition of the shuttle effect, which is considered as a primary shortcoming of Li-S batteries.

3　Conclusions

In summary, Mn_2O_3 hollow spheres were synthesized by using colloidal carbon spheres as the hard template and aimed at the holder for Li-S battery. When the sulfur loading was as high as 51%, the corresponding reversible capacity can remain at 657 mA·g^{-1} after 100 cycle at the current density of 0.9 A·g^{-1}. The rate performance of these Mn_2O_3-S composites were also attractive even at high rate. The good electrochemical performance was mainly contributed by the hollow structure of Mn_2O_3 spheres, which can suppress the volume expansion of sulfur and the sulfides during the charge-discharge process. Importantly, the diffusion of polysulfides could be suppressed effectively by the surface chemical bonding of

Mn_2O_3. The present study confirms the Mn_2O_3 hollow spheres are a promising matrix for Li-S batteries. Further work is in progress.

References:

[1] Chen L, Shaw L L. *J. Power Sources.*, **2014**,**267**:770-783

[2] ZHOU Lan(周兰), YU Ai-Shui(余爱水). *J. Electrochem.*(电化学), **2015**,**21**(3):211-220

[3] Lin Z, Liang C. *J. Mater. Chem. A*, **2015**,**3**:936-958

[4] Manthiram A, Fu Y, Chung, et al. *Chem. Rev.*, **2014**,**114**:11751-11787

[5] Pope M A, Aksay I A. *Adv. Energy Mater.*, **2015**,**5**:1500124

[6] DIAO Yan(刁岩), XIE Kai(谢凯), HONG Xiao-Bin(洪晓斌), et al. *Acta Chim. Sinica*(化学学报), **2013**,**7**(4):508-548

[7] WAN Wen-Bao(万文博), PU Wei-Hua(蒲薇华). *Prog. Chem.*(化学进展), **2013**,**25**(11):1830-1841

[8] He G, Evers S, Liang, et al. *ACS Nano*, **2013**,**7**:10920-10930

[9] Jayaprakash N, Shen J, Moganty S S, et al. *Angew Chem. Int. Ed.*, **2011**,**50**:5904-5908

[10]Qu Y, Zhang Z, Wang, et al. *J. Mater. Chem. A*, **2013**,**1**:14306

[11]Jung D S, Hwang T H, Lee, et al. *Nano Lett.*, **2014**,**14**:4418-4425

[12]Wang M, Zhang H, Wang, et al. *ACS Appl. Mater. Interfaces*, **2015**,**7**:3590-3599

[13]XU Jing-Jing(徐晶晶), LI Bin(李斌), LI Song-Hai(李松梅), et al. *Chinese J. Inorg. Chem.*(无机化学学报), **2015**,**31**(10):2030-2036

[14]Mi K, Jiang Y, Feng J, et al. *Adv. Funct. Mater.*, **2016**,**26**:1571-1579

[15]Ahn W, Lee D U, Song, et al. *RSC Adv.*, **2015**,**5**:29370-29374

[16]Duan X, Han Y, Huang L W, et al. *J. Mater. Chem. A*, **2015**,**3**:8015-8021

[17]MAO Yan(毛艳), ZHANG Chuan-Hui(张传辉), ZHANG Yang(张杨), et al. *Chinese J. Inorg. Chem.*(无机化学学报), **2013**,**29**(5):889-895

[18]Li J, Ding B, Xu G, et al. *Nanoscale*, **2013**,**5**:5743-5746

[19]Wei S Z, Li W Y, Cha J J, et al. *Nat. Commun.*, **2013**,**4**:1331

[20]Choi Y J, Jung B S, Lee, et al. B. *Phys. Scr.*, **2007**,**T129**:62-65

[21]Li W, Hicks-Garner J, Wang J, et al. *Chem. Mater.*, **2014**,**26**:3403-3410

[22]Liang X, Hart C, Pang Q, et al. *Nat. Commun.*, **2015**,**6**:5682

[23]Wang X, Li G, Li J, et al. *Energy Environ. Sci.*, **2016**,**9**:2533-2538

[24]Sun X, Li Y. *Angew. Chem. Int. Ed.*, **2004**,**43**:597-601

[25]Bongu C S, Karuppiah S, Nallathamby K, et al. *J. Mater. Chem. A*, **2015**,**3**:23981-23989

[26]Kolathodi M S, Rao S N H, Natarajan T S, et al. *J. Mater. Chem. A*, **2016**,**4**:7883-7891